How a responsive reproduction factor is determinant in a prey-predator dynamics: A numerical and analytical study in a discrete-time model

Cite as: Chaos 35, 013154 (2025); doi: 10.1063/5.0239007 Submitted: 16 September 2024 · Accepted: 5 January 2025 · Published Online: 27 January 2025











M. S. Bittencourt, 1 📵 E. L. Brugnago, 1,a) 📵 Z. O. Guimarães-Filho, 1 📵 I. L. Caldas, 1 📵 and A. S. Reis 1,2 📵





AFFILIATIONS

- ¹Physics Institute, University of São Paulo, 05508-090 São Paulo, SP, Brazil
- ²Institute of Science and Technology, Federal University of São Paulo, 12247-014 São José dos Campos, SP, Brazil

Note: This paper is part of the Focus Issue, From Sand to Shrimps: In Honor of Professor Jason A. C. Gallas.

a)Author to whom correspondence should be addressed: eduardolbrugnago@gmail.com

ABSTRACT

In this work, we investigate the dynamics of a discrete-time prey-predator model considering a prey reproductive response as a function of the predation risk, with the prey population growth factor governed by two parameters. The system can evolve toward scenarios of mutual or only of predators extinction, or species coexistence. We analytically show all different types of equilibrium points depending on the ranges of growth parameters. By numerical study, we find the occurrence of quasiperiodic, chaotic, and hyperchaotic behaviors. Our analytical results are corroborated by the numerical ones. We highlight Arnold tongue-like periodic structures organized according to the Farey sequence, as well as pairs of twin shrimps connected by two links. The mathematical model captures two possible prey responsive strategies, decreasing or increasing the reproduction rate under predatory threat. Our results support that both strategies are compatible with the populations coexistence and present rich dynamics.

Published under an exclusive license by AIP Publishing. https://doi.org/10.1063/5.0239007

Models of interspecific interactions are widely studied in the context of dynamical systems, with special interest in understanding the influence of control parameters on ecological relationships. Simplified descriptions, involving two species, are among the paradigmatic systems, such as the continuous time Lotka-Volterra model of two interacting populations. Discretetime versions appear as a good simplification of these models, focusing the study of dynamics. Proposed variations include adaptations of species to environmental conditions, addition of variables, and analytical simplifications, from which discretetime systems can be derived. In this study, we consider a non-linear discrete-time prey-predator model with a prey reproductive response to the predatory risk. We include a reproduction factor depending on the predator population, which can simulate both the increase or decrease in prey reproduction in the face of a greater threat of predation. Such a responsive function adds another non-linearity to the system and enriches the dynamics.

I. INTRODUCTION

Since Malthus proposal on the mismatch between human population growth and food resources,1 several mathematical formulations have been considered to describe population dynamics. The Malthusian model assumes a demographic growth rate proportional to the population itself,^{2,3} i.e., follows a geometric progression. Such behavior had already been proposed by Euler in a previous publication.4 Verhulst conceived a variation on the exponential model, considering that a given population cannot grow indefinitely,5,6 as there must be natural inhibitions to its increase. In these studies, Verhulst expresses the logistic growth equation.³ Both models deal with isolated population dynamics, without interspecific interaction. However, in nature, there is competition for resources between different species in a given environment, as well as predation relationships.⁷⁻⁹ Studying population dynamics taking into account interspecific interactions is fundamental to understanding coexistence and preservation¹⁰

scenarios, distinguishing them from those that could lead to species extinction.

To address the problem of interaction between two species, Lotka^{11,12} and Volterra^{13,14} independently proposed a differential equation system to describe competition (Lotka) and predation (Volterra). Then, known as the Lotka–Volterra^{15,16} model (LV), this two variable system is given by

$$\dot{x} = Ax - Bxy,
\dot{y} = Dxy - Cy,$$
(1)

where A and C are the exponential growth (decrease) parameters, while B and D are the interaction ones. The variables x and y represent each species population or the corresponding densities. In a prey–predator approach, the first variable refers to the prey and the second to the predator population, with real positive parameters. As a paradigmatic model, the original LV and its variations are widely studied, even extended to more interacting species increasing the system's dimension.

One can consider a slightly different approach than the classical LV, in which the intrinsic population dynamics is given by a logistical function. Such kind of model includes species internal competition. An example is a three-variable system, using the logistic term for prey only and with predator dominance, which show chaotic behavior in widebands of the parameter space. These competition models go beyond ecological relationships, being used with additional terms in studies about tumor growth. Is, I In this context, Gallas *et al.* Show that a model of three-cell cancer population presents chaotic dynamics, finds shrimp spirals, and demonstrates an intricate isospike counting formation rule within periodic domains.

Another approach to modeling population dynamics is to describe it by means of difference equations. Similar to Verhulst's expression, the logistic map²¹

$$x_{n+1} = ax_n(1 - x_n) (2)$$

includes a quadratic decrement term, providing an inhabitant upper limit. Variable $x_n \in [0,1]$ represents the population density, or the normalized size, at nth iteration, while the growth parameter is $a \in [0,4]$. After May's review,²¹ quadratic maps–specially, the logistic family–has been deeply investigated, and its rich dynamics and characteristic universalities are known.^{22–25} This system had been considered in other contexts,²⁶ e.g., the Ulam and Von Neumann's proposal²⁷ of a pseudorandom number generator in the form $x_{n+1} = 4x_n(1-x_n)$.

Two-population models can be obtained by coupling logistic maps, representing species interactions in many scenarios. ^{28–30} In these systems, for certain parametric configurations, there is multistability of periodic solutions, as well as the coexistence of chaotic and periodic attractors. Furthermore, Neimark–Sacker bifurcations ³¹ are shown to occur, leading to quasiperiodic regimes. ^{32,33} Arnold tongues and shrimp-shaped domains are also found. ³³ Discrete-time versions of LV are other types of simplified models for some contexts, ^{34–36} which may include logistical terms. ³⁷ A diversity of such systems results from different discretization methods.

A prominent topic in ecological systems is the response of a given species depending on the density (or size) of another, as in cases of predator's reproduction rate and behavior affected by prey density.^{38,39} In this regard, numerical and functional responses^{40,41} are used to model changes in predator's population growth and consumption rate as a function of prey density. It is evidenced in the recent literature that the presence of predators can also lead to population responses in prey, reducing reproduction and increasing mortality from other factors.⁴² Anti-predation behavior has a cost for the prey population,⁴³ which can even affect reproductive aspects. This type of behavior includes diverse prey activities, which can range from avoiding the predator through group vigilance and alertness, to escape and fighting for survival. The predator-induced breeding suppression significantly impacts the prey-predator system dynamics, as observed in small mammal populations under such effect.44,45

In this work, we study a discrete-time prey-predator model with the prey population growth depending on the density of predators. Based on a discrete-time LV model, ^{34,46} we modify the prey logistic parameter, inserting a functional variation in response to the predator presence in the environment. In Sec. II, we discuss the modified model, followed by an analysis of its equilibrium point stability, covered in Sec III. Numerical results are presented in Sec. IV, where we investigate the dynamics of the proposed prey-predator system as a function of base and responsive growth parameters. In Sec. V, we summarize the main results and present our considerations about the influence of prey growth responsiveness on prey-predator dynamics.

II. MODEL

Based on recent research studies about prey reproductive responses to predation risk^{42,45} and inspired by a discrete-time prey–predator model studied by Danca *et al.*,⁴⁶ we propose a change in the prey population growth. In this system, a logistic term is assumed for the prey density evolution, while for predators, there is direct dependence on predatory interaction, as follows:

$$x_{n+1} = ax_n(1 - x_n) - bx_n y_n,$$

 $y_{n+1} = dx_n y_n.$ (3)

Variables x_n and y_n are relative to the prey and predator, respectively. The interaction parameters b and d are similar to those in LV.

Our approach is to replace the growth parameter a with the factor

$$\alpha(y_n; a_0, a_r) := a_0 + (a_r - a_0) \frac{y_n^2}{1 + v_n^2},$$
 (4)

including a dependency on y_n . The original model (3) is recovered by making $a_0 = a_r = a$, where the parameter a_0 is the base growth and a_r the responsive one. Small amounts of predators in the environment bring the prey growth factor close to the base value, while larger predator numbers accentuate responsive behavior. With $a_r < a_0$, we model the prey reproduction decrease given a greater risk of predation, as observed in nature. However, with $a_r > a_0$, we consider an alternative strategy, whereby prey increases the reproduction rate in response to greater threats. The nonlinear

part of the growth factor is in the form of a Holling type III functional response.^{47,48} Although it is not a functional response, which is defined to ecological models as the rate of prey consumption by predators dependent on prey density.^{40,41}

The modified model is given by

$$x_{n+1} = \alpha(y_n; a_0, a_r) x_n (1 - x_n) - b x_n y_n,$$

$$y_{n+1} = d x_n y_n,$$
 (5)

where all parameters are positive real numbers and $a_0, a_r \in (0, 4]$. The variables fall within the validity domains $x_n \in [0, 1]$ and $0 \le y_n$. Throughout this text, we refer to system (5) as the responsive prey–predator or simply as the responsive model.

Figure 1 shows a chaotic attractor of the responsive model with interaction parameters b=0.2 and d=3.5, being the growth ones $a_0=1.5$ and $a_{\rm r}=4.0$. This is an example of dynamics arising from the strategy of increasing reproduction when the threat of predation enlarges. We adopt the initial condition $(x_0,y_0)=(0.1,0.01)$ and discard a transient of 10^5 interactions. The same values of the interaction parameters and the initial condition, but with another growth pair $(a_0,a_{\rm r})$, result in different dynamics as illustrated in Fig. 2. The hyperchaotic attractor shown in panel Fig. 2(a) is obtained for $a_0=a_{\rm r}=3.9$, reducing the model to non-responsive. This attractor is reproduced from Danca's work.⁴⁶ The other three panels depict dynamics with $a_{\rm r}< a_0$, being the prey's behavior of reducing population growth in the face of a predator's greater number.

We kept the base growth $a_0 = 3.9$ and chose three values for a_r , from which we obtain the orbits portrayed in Figs. 2(b)-2(d).

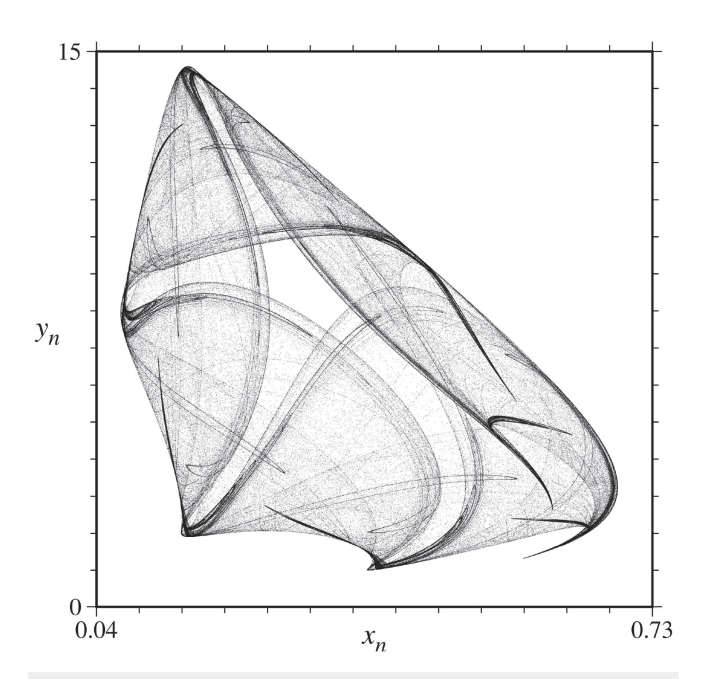


FIG. 1. Chaotic attractor of the responsive model (5) with the parameters $(a_0, a_{\rm f}, b, d) = (1.5, 4.0, 0.2, 3.5)$. Lyapunov spectrum $(\lambda_1, \lambda_2) = (0.077, -0.201)$. Adopted the initial condition $(x_0, y_0) = (0.1, 0.01)$ and discarded the first 10^5 iterations as transient.

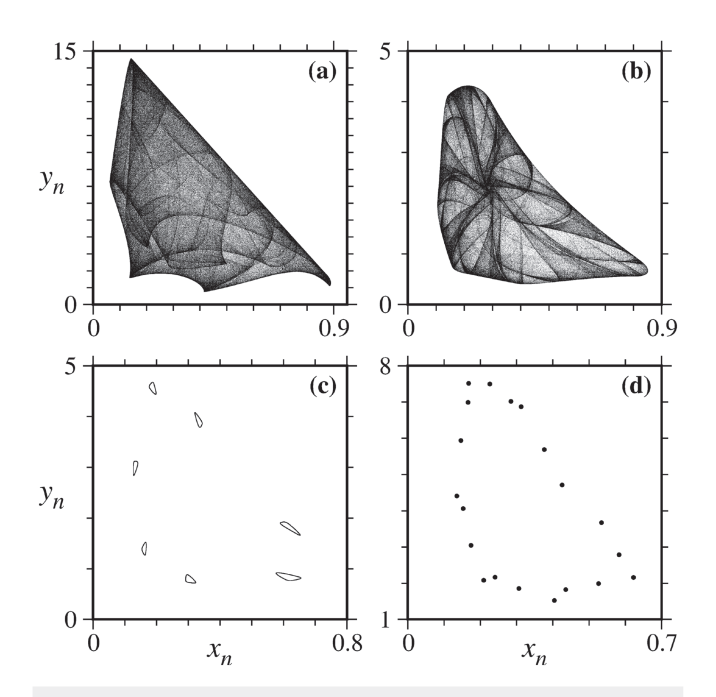


FIG. 2. Attractors of the responsive model (5) with the parameters $(a_0, b, d) = (3.9, 0.2, 3.5)$. Adopted the initial condition $(x_0, y_0) = (0.1, 0.01)$ and discarded the first 10^5 iterations as transient. Hyperchaotic attractors for (a) $a_r = 3.9$, with Lyapunov spectrum $(\lambda_1, \lambda_2) = (0.189, 0.119)$; and (b) $a_r = 1.7$, with $(\lambda_1, \lambda_2) = (0.081, 0.031)$. (c) Quasiperiodic for $a_r = 1.9$. (d) Period-20 for $a_r = 2.755$.

Panel (b) illustrates a hyperchaotic attractor, given $a_{\rm r}=1.7$. Note that the dynamics shown in panels (a) and (b) differ only by the inclusion of the responsive term. For panel (c), we adopted $a_{\rm r}=1.9$ and, with such a configuration, the system presents quasiperiodic behavior. This attractor arises from a Neimark–Sacker bifurcation of a period-7 orbit. The occurrence of these bifurcations is discussed in Sec. IV. The last panel, Fig. 2(d), shows a period-20 attractive orbit obtained with $a_{\rm r}=2.755$. The different regimes achieved according to the responsive parameter are also subject of Sec. IV.

III. ANALYTICAL RESULTS

Prey–predator systems, such as models (3) and (5), can evolve to one of three scenarios, namely, (i) mutual extinction, (ii) extinction of predators only, and (iii) coexistence. Mutual extinction is the equilibrium point $E_{\rm ext}(0,0)$, whose stability is analyzed in Subsection III B. Note that if prey vanishes, predators become extinct in the next iteration (generation).

Scenario (ii) presents the logistic map dynamics, in which the prey population survives alone. In this circumstance, the factor (4) is reduced to the base growth. It is trivial that $d \le 1$ is sufficient to the asymptotic extinction of predators. However, a necessary and sufficient condition to lead to this scenario is more general and involves growth parameters. Finally, considering any trajectory in scenario (iii), by writing y_{n+2} in terms of x_n and y_n in Eqs. (5), we obtain

an upper population quota for predators. This is done by analyzing the first and second partial derivatives of y_{n+2} with respect to both variables. Assuming a transient evolution of $m \ge 0$ iterations, we found

$$y_{n>m} \le \frac{\left(da_{\max}\right)^2}{64h}, \text{ with } a_{\max} = \max\{a_0, a_r\}.$$
 (6)

Such a result presumes that the prey population remains in the unitary domain.

A. Equilibrium points

From the fixed-point assumption for discrete-time systems $E(x_*,y_*)=(x_{n+1},y_{n+1})=(x_n,y_n)$, we obtain the period-1 orbits for all three scenarios listed previously. Mutual extinction is the trivial equilibrium $E_{\rm ext}(0,0)$, as mentioned earlier. Another type of fixed point is found in scenario (ii), for which the first equation of system (5) reduces to the logistic map, thus the solutions depending on the base growth parameter in the same way as that. This equilibrium is denoted by $E_{\rm log}(1-1/a_0,0)$.

Scenario (iii) is characterized by the predator species survival, i.e., the corresponding equilibrium coordinate $y_* \neq 0$. Such a fact results in $x_* = 1/d$. Given the restricted interval $x_* \in [0,1)$, solutions found in this scenario are only valid when d > 1. As for the predator population, from the first equation of system (5), we obtain

$$P(y) = y^3 + Ry^2 + y + B, (7)$$

whose coefficients are described by the function

$$\mathcal{F}(a,b,d) = \frac{1}{b} \left[1 - a \left(1 - \frac{1}{d} \right) \right],\tag{8}$$

with $R = \mathcal{F}(a_r, b, d)$ and $B = \mathcal{F}(a_0, b, d)$. In the fixed point, it is verified as $P(y_*) = 0$. The number of solutions with a physical sense depends on the R and B range. If both $R, B \geq 0$, equivalent to $a_0, a_r \leq d/(d-1)$, no equilibrium points are found with the predator survival, given that for this configuration, the polynomial (7) has no positive real roots. Next, we only discuss parameter intervals in which valid solutions $y_* \in \mathbb{R}_+$ exist.

The simplest case is B=0, which corresponds to the model parameters $a_0=d/(d-1)$, resulting in only two equilibrium points,

$$E_{B=0}^{\pm} \left(\frac{1}{d}, \frac{-R \pm \sqrt{R^2 - 4}}{2} \right).$$
 (9)

These solutions are valid for $(1+2b)a_0 \le a_r$, into the prey strategy of increasing reproduction as response to a high predation risk. In particular, when $(1+2b)a_0 = a_r$, there is a single point $E_{B=0}\left(1/d,1\right) = E_{B=0}^- = E_{B=0}^+$.

The second case is B > 0, whose base growth parameter $a_0 < d/(d-1)$. It follows that R < 0 is a necessary condition for the existence of period-1 orbits with non-zero predator population. This configuration figures in the same reproductive strategy as the previous case. Therefore, the polynomial (7) has positive real roots

iff $P(y_{\min}) \le 0$, where the abscissa

$$y_{\min} = \frac{-R + \sqrt{R^2 - 3}}{3} \tag{10}$$

corresponds to the curve local minimum. In order to simplify the resolution, we define the upper boundary $B_+ := B - P(y_{\min})$ of B, or explicitly,

$$B_{+} := \frac{9R - 2R^{3} + (2R^{2} - 6)\sqrt{R^{2} - 3}}{27}.$$
 (11)

Using the above value, it is shown that valid fixed-point solutions are only obtained in the interval

$$\max \left\{ 0, \left[1 - bB_{+} \right] \frac{d}{d-1} \right\} \le a_{0} < \frac{d}{d-1}. \tag{12}$$

Note that the range in (12) relates the two growth parameters. From $0 < B \le B_+$, we also obtain the corresponding relation to the responsive parameter,

$$(1+2b)\frac{d}{d-1} < a_{\rm r}. (13)$$

See that R = -2 results in $B_+ = 0$, returning to the particular solution $E_{B=0}$ of the case B = 0.

Mutually respecting the intervals (12) and (13), the case B > 0 presents the following two equilibrium points:

$$E_{B>0}^{\pm} \left(\frac{1}{d}, y_{\min} \pm \delta_{\pm} \right), \tag{14}$$

which are described in terms of the local minimum coordinate shown in Eq. (10). It is important to note that, in general, $\delta_+ \neq \delta_-$, and equality is verified iff $B = B_+$, with both $\delta_\pm = 0$. Thus, the solutions reduce to the single one fixed point $E_{B>0}(1/d,y_{\min})$. To determine exactly y_* for $0 < B < B_+$, the Cardano–Tartaglia method ⁴⁹ for general cubic equations is used.

The last case is B < 0, with $a_0 > d/(d-1)$. For a large domain in parameter space, there is always one solution. Three valid equilibrium points only occur in the range

$$\left[1 - \min(0, B_{+})b\right] \frac{d}{(d-1)} < a_{0} < (1 - bB_{-}) \frac{d}{(d-1)}$$
and $(1 + \sqrt{3}b) \frac{d}{(d-1)} < a_{r}$. (15)

The B_{-} edge is given by

$$B_{-} := \frac{9R - 2R^3 - (2R^2 - 6)\sqrt{R^2 - 3}}{27},\tag{16}$$

obtained in the same way of B_+ , but from the $y_{\rm max}$ coordinate of the polynomial's local maximum. Within the region (15), $B_+ < 0$ solely in the narrow interval $-2 < R < -\sqrt{3}$. In particular, when $B = B_-$ (or $B = B_+$), there are just two fixed points. We obtain y_* of $E_{B<0}$ through the general expression for the roots of cubic polynomials. This case presents configurations in both responsive reproduction strategies.

We classify the single solution subcases according to

- (a) $E_{B<0}^{a}$ when $a_{r} < (1 + \sqrt{3}b) \frac{d}{(d-1)}$,

(b)
$$E_{B<0}^b$$
 when $(1+\sqrt{3}b)\frac{d}{(d-1)} < a_r$ and $(1-bB_-)\frac{d}{(d-1)} < a_0$, and (c) $E_{B<0}^c$ when $(1+\sqrt{3}b)\frac{d}{(d-1)} < a_r < (1+2b)\frac{d}{(d-1)}$ and $\frac{d}{(d-1)} < a_0 < (1-bB_+)\frac{d}{(d-1)}$.

The triple solution points consists of a pair $E_{B<0}^\pm$, presenting the same form of (14), and $E_{B<0}^0$, with $y_* < y_{\rm max}$.

B. Stability of equilibrium points

In the following, we analyze the asymptotic stability of the equilibrium points found in scenarios (i) and (ii). To this end, we obtain the eigenvalues ξ_i of the Jacobian matrix of system (5) calculated at each point studied. For discrete-time systems, if $|\xi_i| < 1 \,\forall i$, then the fixed point is attractive.51

The Jacobian evaluated at any $E(x_*, y_*)$ is given by

$$\mathbb{J}\Big|_{E} = \begin{bmatrix} \alpha|_{y_{*}}(1-2x_{*}) - by_{*} & \alpha'|_{y_{*}}x_{*}(1-x_{*}) - bx_{*} \\ dy_{*} & dx_{*} \end{bmatrix},$$

where $\alpha \equiv \alpha(y_n; a_0, a_r)$, as defined in Eq. (4), and its derivative is with respect to y_n ,

$$\alpha'|_{y_*} = \left. \frac{\partial \alpha}{\partial y_n} \right|_{y_*} = \frac{2(a_r - a_0)y_*}{(1 + y_*^2)^2}.$$
 (17)

The characteristic polynomial $P(\xi) = \xi^2 - T\xi + D$ of a \mathbb{J} matrix can be written in a general form, explicitly specifying the fixed-point

$$P(\xi) = \xi^{2} - \left[\alpha|_{y_{*}}(1 - 2x_{*}) - by_{*} + dx_{*}\right]\xi + dx_{*}\left[\alpha|_{y_{*}}(1 - 2x_{*}) - \alpha'|_{y_{*}}y_{*}(1 - x_{*})\right].$$
(18)

For the mutual extinction scenario $E_{\text{ext}}(0,0)$, one eigenvalue is null and the other $\xi_{\text{ext},2} = a_0$. Therefore, the extinction of both species is determined solely by the base growth parameter. Thus, $E_{\rm ext}$ is an attractive equilibrium point in the interval $0 \le a_0 < 1$. For the second scenario, in which only the prey population survives, the stability of point $E_{log}(1-1/a_0,0)$ is also determined exclusively by the base growth parameter. Given the eigenvalues $\xi_{\log,1} = 2$ a_0 and $\xi_{\log,2} = d(1-1/a_0)$, E_{\log} is attractive in the range $1 < a_0$ $< \min[d/(d-1), 3].$

In scenario (iii), the coefficients of the characteristic polynomial take the form

$$T = \frac{(2 - a_0/d) + (2 - a_r/d)y_*^2}{1 + y_*^2},$$

$$D = \frac{(1 - 2/d) \left[a_r y_*^4 + (a_0 - a_r)y_*^2 + a_0 \right]}{\left(1 + y_*^2 \right)^2} + \frac{2a_0(1 - 1/d)y_*^2}{\left(1 + y_*^2 \right)^2}.$$

Given these terms, $\xi_- < 1$ and $\xi_+ > -1$ are verified since both eigenvalues are real numbers, regardless of the fixed-point coordinates in this scenario. Thus, an equilibrium $E(1/d, y_*)$ is stable iff T - D < 1 and -1 < T + D, for $0 \le T^2 - 4D$. While, case $T^2 - 4D < 0$, a fixed point is stable iff D < 1. A complete analysis of the fixed-point stability is extensive and is not the focus of this work. We chose to omit a detailed description, and in Sec. IV, we explore the numerical results.

IV. NUMERICAL RESULTS

In this section, we numerically investigate the system's dynamics as a function of the population growth parameters. The other two constants were set at b = 0.2 and d = 3.5. For all simulations, we adopt the initial condition $(x_0, y_0) = (0.1, 0.01)$ and discard 2×10^5 iterations as transient, after which we consider 106 iterations to compute the Lyapunov spectrum,⁵¹⁻⁵³ constituted by the ordered exponents $\lambda_1 \geq \lambda_2$. The orbit periodicity was verified by simultaneously checking the largest Lyapunov exponent and the period-p count of each solution obtained. We also distinguish chaotic behavior, with $\lambda_1 > 0$ and $\lambda_2 < 0$, from the hyperchaotic⁵⁴ kind characterized by both $\lambda_{1,2} > 0$.

Figure 3 exhibits the parameter plane $a_r \times a_0$ in the intervals $a_{\rm r}, a_0 \in (0, 4]$. The color scheme discriminates periodic domains from the quasiperiodic (gray), chaotic (black), and hyperchaotic ones (dark-purple). From $a_0 \approx 3.25$ with small values of a_r (left bottom corner), the system evolves to $x_n < 0$, loses ecological meaning, and leads to divergence (white). Between the vast period-1 (blue color) and the chaotic region, there is a broad band of quasiperiodicity in which Arnold tongue-like periodic structures are inserted. Following the a_r decrease direction, a sequence of periods is given by incrementing the values of primary tongues by one unit, e.g., from

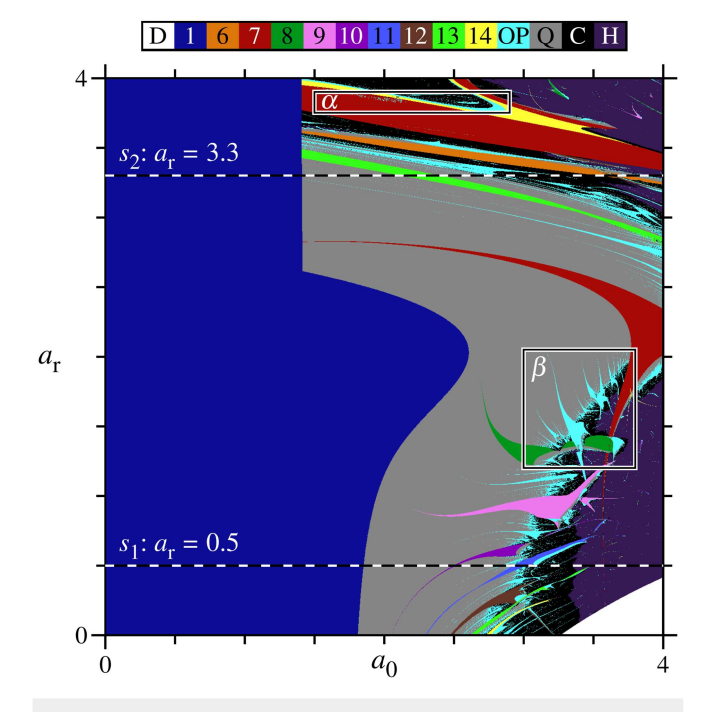


FIG. 3. Parameter plane $a_r \times a_0$ discretized in a uniform grid of 1200 \times 1200 points, with $a_r, a_0 \in (0, 4]$. The color scheme distinguishes regions of periodic behavior, whose periods are numbered, from quasiperiodic (Q), chaos (C), hyperchaos (H), and divergency (D). Other periods (OP) greater than 14 are all in cyan. Intermediate counts, between 1 and 6, are not observed. Note the periodic areas, such as Arnold tongue shapes, inserted in the quasiperiodic band. Along the dashed lines, s_1 and s_2 are the bifurcation diagrams shown in Fig. 8. The boxes α and β are magnified in Figs. 4 and 5, respectively.

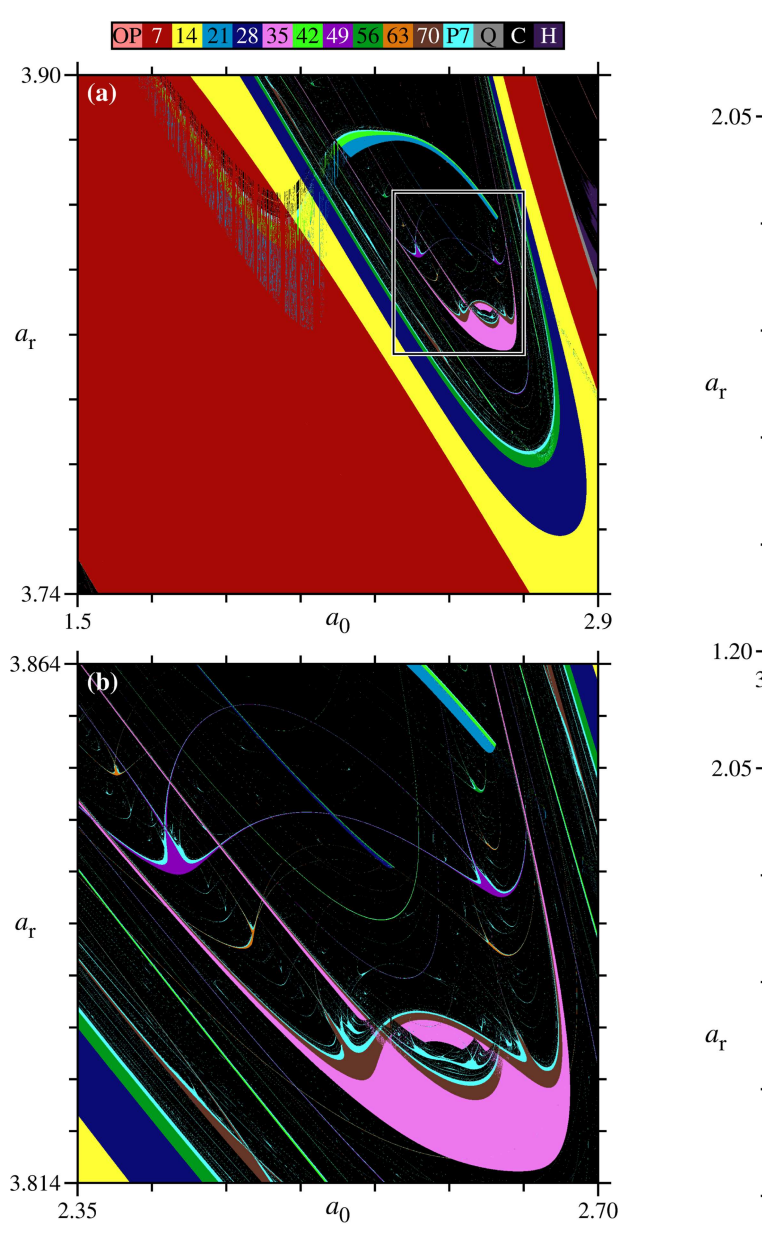


FIG. 4. Parameter plane discretized on a uniform grid of 1600×1600 points, with the axis intervals open to the left. In both panels, periods according to a numbered color code, where the unlisted multiple of 7 (P7) are represented in cyan, and other periods (OP) in salmon color. Quasiperiodic (Q), chaotic (C), and hyperchaotic (H) behaviors are also distinguished. (a) Magnification of region α in Fig. 3. Periods multiple of 7 are predominant. (b) Enlargement of the highlighted box in the top panel. Pairs of same periods shrimp appear symmetrically connected by two links.

period-7 (red) to 8 (green), 9 (pink), 10 (violet color), and onward. As typical of similar formations, the general period's rule is according to the denominators in Farey sequences,^{55–57} this covers all tongues found in a quasiperiodic zone. Thus, the period of an

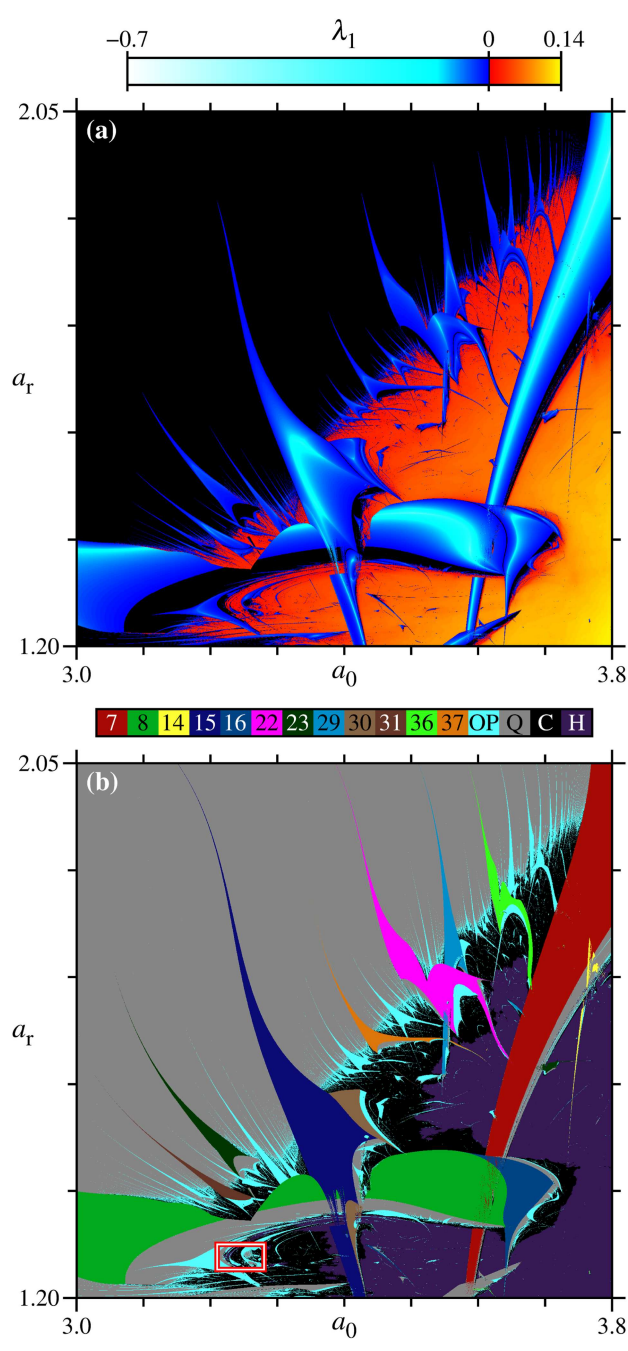


FIG. 5. Parameter plane discretized on a uniform grid of 1600×1600 points, with the axis intervals open to the left. Both panels present results across the region β in Fig. 3. (a) Largest Lyapunov exponent on color gradient, with $\lambda_1=0$ in black color. This quantity was obtained with an accuracy of 1×10^{-4} . (b) Periods according to a numbered color code, where the other periods (OP) are represented in cyan. Quasiperiodic (Q), chaotic (C), and hyperchaotic (H) behaviors are also distinguished. Note the Arnold tongue-like periodic structures, inserted in the quasiperiodic band, and advancing toward chaotic ones. The highlighted box is enlarged in Fig. 6.

intermediate structure is the sum of adjacent lower-order ones. The highlighted box β is enlarged in Fig. 5, where details of the region are shown. Seeing the period-13 tongue (light green) between the p=7 one and the p=6 area (orange color), we infer that this last strip is part of the sequence. Above the large quasiperiodic zone is a period-7 structure, which folds to period-14 (yellow) and engulfs a chaos area, where only period-7k shrimps 58,59 appear. The region α is detailed in Fig. 4. A hyperchaotic domain is beyond the chaos band, in which periodic structures advance and other immersed ones are found, such as periods 8 and 9 in the upper right corner of Fig. 3.

Figure 4(a) magnifies the area α highlighted in Fig. 3. The inner contour of the period-14 strip delimits a region where all non-chaotic orbits are of period multiples of 7. This is fully integrated into the prey's alternative strategy of increasing reproduction due to the greater risk of predation. Following the period-doubling cascade from 7 (red) \rightarrow 14 (yellow) \rightarrow 28 (dark blue) \rightarrow 56 (dark green) \rightarrow etc., there is a chaotic region in which connected shrimps are immersed. In addition to the approximately parabolic curve around this area of chaos, it is closed by a periodic band near $a_{\rm r}=3.86$, with doubling from p=21 (light blue). Periods greater than 70 and multiples of 7 are in cyan (P7). Points of other periods (OP), vestigial on the outside of the p=7k region, are in salmon color. The period-doubling cascade band from p=21 overlaps with the cascade from p=7 for $3.82 < a_{\rm r}$ and $1.7 < a_0 < 2.2$. The rarefied aspect at this intersection is associated with multistability.

Figure 4(b) panel enlarges the outlined box in Fig. 4(a), where the links between the twin shrimps are seen. Both the internal chaotic region and the periodic domains immersed in it originate from the opening of a period-7 structure, a phenomenon that occurs with the variation of the parameter d. In the literature, shrimps connected by alternating "antennas" are also found. 60,61 Here, we

present an example of these symmetrically connected forms, i.e., sharing the boundary bifurcation curve between chaos and the main body ("head" or anterior part) of the same period shrimps pairs, establishing a link between the twins. There is a second connection established by the saddle-node bifurcation curve that delimits the posterior "antennas," as seen in the period-49 twin shrimps (violet color). The fused structure of period-35 (pink) provides an idea about how the twin shrimp formation process works: As the main bodies separate, connections remain through common bifurcation curves.

Shapes similar to Arnold tongues are displayed in Fig. 5, which magnifies the region β highlighted in Fig. 3. Panel (a) represents in colors the largest Lyapunov exponent calculated along the orbits obtained for each point on the parameter plane grid. Periodic solutions are in shades of blue ($\lambda_1 < 0$), and chaotic and hyperchaotic ones are in the warm color gradient ($\lambda_1 > 0$). Distinction between chaos and hyperchaos is made in panel (b). The case $\lambda_1 = 0$ (black) was obtained with high accuracy, corroborating a precise distinction of the quasiperiodic behavior. Tongues appear in the broad quasiperiodic band, and the periodic structure enters the chaotic region. In several of these, a bifurcation creates a new quasiperiodic band with smaller tongues inserted, which follow the same pattern, generating a cascade. As an example, see the structure in the lower left corner, in the approximate range $1.20 < a_{\rm r} < 1.37$ advancing in such a cascade from $a_0 = 3$ to $a_0 \approx 3.22$.

Figure 5(b) depicts the period count in a color code, also distinguishing between the non-periodic solutions. The Arnold tongue-like structures are organized according to the denominators of fractions in a Farey sequence, a well-known period formation rule. In this way, the period of an intermediate tongue is given by the sum of the adjacent ones, respecting the succession of Farey

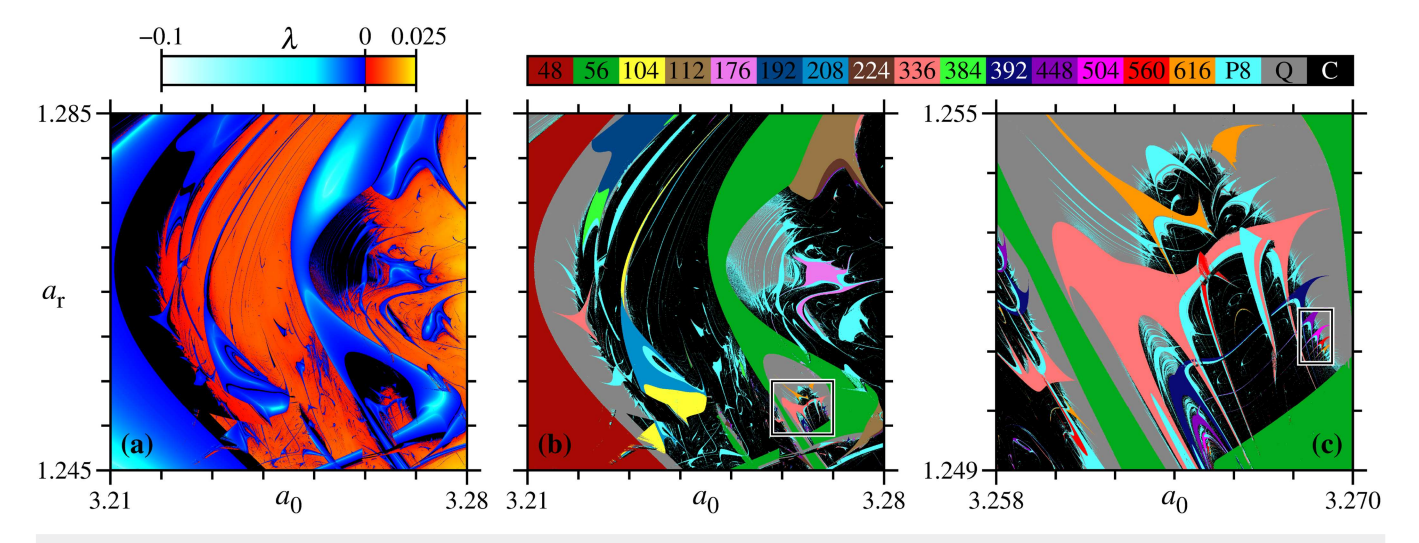


FIG. 6. Parameter plane discretized on a uniform grid of 1600×1600 points, with the axis intervals open to the left. The region in panels (a) and (b) corresponds to the highlighted box in Fig. 5(b). (a) Largest Lyapunov exponent on color gradient, with $\lambda_1 = 0$ in black color. This quantity was obtained with an accuracy of 1×10^{-4} . (b) Periods according to a numbered color code, where the unlisted p = 8k (P8) are represented in cyan. For simplicity, we group chaos and hyperchaos under the same label (c). Quasiperiodic (Q) behaviors are distinguished. In this range, there are only periods multiples of 8. (c) Enlargement of the region delimited in the lower left corner of panel (b). Connected Arnold tongue pairs are observed, whose links pass through the central chaotic region. The highlighted box near the right margin is enlarged in Fig. 7(a).

sequences, as follows:

$$F_{1} = \left\{ \frac{0}{1}, \frac{1}{1} \right\},$$

$$F_{2} = \left\{ \frac{0}{1}, \frac{1}{2}, \frac{1}{1} \right\},$$

$$F_{3} = \left\{ \frac{0}{1}, \frac{1}{3}, \frac{1}{2}, \frac{2}{3}, \frac{1}{1} \right\},$$

$$F_{4} = \left\{ \frac{0}{1}, \frac{1}{4}, \frac{1}{3}, \frac{2}{5}, \frac{1}{2}, \frac{3}{5}, \frac{2}{3}, \frac{3}{4}, \frac{1}{1} \right\},$$

$$\vdots$$

$$F_{k} = \left\{ \frac{0}{1}, \frac{1}{k}, \dots, \frac{1}{2}, \dots, \frac{k-1}{k}, \frac{1}{1} \right\}.$$

Each F_k above is a Farey sequence, ⁵⁵ formed by all reduced fractions i/j, with $i, j \le k$. Taking three successive fractions p_{n-1}/q_{n-1} , p_n/q_n , and p_{n+1}/q_{n+1} within the k-th sequence, in the minimal form, it is verified that

$$\frac{p_n}{q_n} = \frac{p_{n-1} + p_{n+1}}{q_{n-1} + q_{n+1}}. (19)$$

As seen in Fig. 3, in the direction of decreasing the responsive parameter, the primary tongues succeed in increments of one unit. In panel (b), we present the interval between the structures of period-7 (red) and 8 (green), where the period-15 one (dark blue) is located. From p = 7 and p = 15, we get the tongue of period-(7 + 15) = 22 (magenta). Subsequently, in the direction of increasing a_0 and a_r , there are the structures of period p = 7 + 22 = 29 (light blue) and p = 7 + 29 = 36 (light green), similarly in the decreasing direction of parameters. Note that rule is universal, covering all tongues, even those of periods not discriminated in the figure (OP in cyan). We observe that the tongues of periods-8 and 15 do not end only with the bifurcation to quasiperiodic behavior, also presenting period-doubling directions. As examples, the two p = 30regions (light brown) that arise near $a_0 = 3.4$ from the p = 15 structure. Furthermore, the small insertion of period-14 advancing over the period-7 band and passing through the quasiperiodic one, near $a_0 = 3.75$ and $a_r = 1.71$, indicates multistability both between p = 7and p = 14, as well as periodic and aperiodic behaviors. Finally, we see that the hyperchaos area (purple) advances into the chaotic strip with irregular boundaries.

The box highlighted in Fig. 5(b) is explored in detail in Fig. 6. For simplicity, we chose not to distinguish hyperchaos from chaos in the next magnification. Panel (a) depicts the largest Lyapunov exponent in colors according to the legend. The meaning of the colors is the same as that adopted in Fig. 5(a) with due scale adjustment. We obtain $\lambda_1 \approx 0$ (black) with high accuracy, but the period-doubling bifurcation curves appear broadened given the small values of $|\lambda_1|$. For example, at $a_r \approx 1.275$ and around $a_0 = 3.225$. The broad black color regions in (a) are confirmed quasiperiodic (gray) in panel (b), where the color code distinguishes the periodic and aperiodic regions. In the selected range $1.245 < a_r \leq 1.285$ and $3.21 < a_0 \leq 3.28$, all periodic orbits are of the form p = 8k. This is related to the cascade $p = 8 \rightarrow Q \rightarrow p = 48 \rightarrow Q \rightarrow$, etc., which starts in

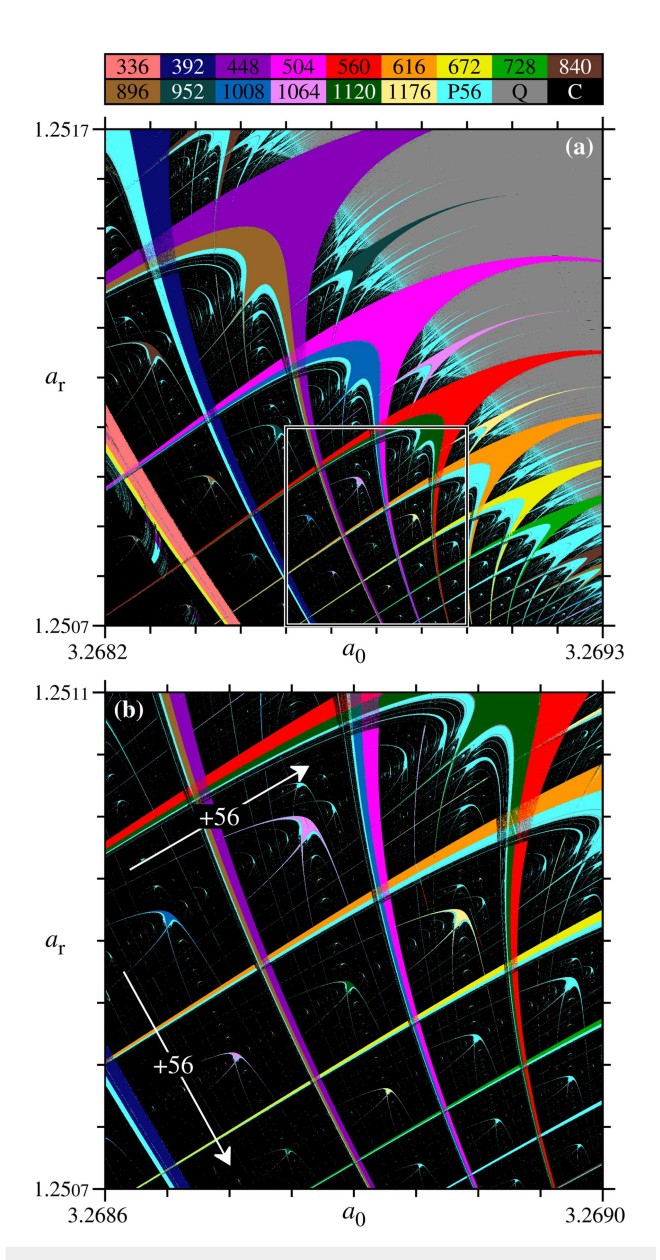


FIG. 7. Parameter plane discretized on a uniform grid of 1600×1600 points, with the axis intervals open to the left. In both panels, periods according to a numbered color code, where the unlisted multiples of 56 (P56) are all represented in cyan. Quasiperiodic (Q) and chaotic (C) behaviors are also distinguished. (a) Magnification of the region highlighted in Fig. 6(c). The megastructure, similar to a fishing net, is here called a "shrimp fisher." (b) Enlargement of the bottom central box in the top panel. Shrimps immersed in the chaotic domains, enclosed by the periodic grid, follow a rule of period addition in two directions, as indicated by arrows.

the period-8 tongue present in the left bottom corner of Fig. 5(b). Such a structure partially contours the chaotic region subsequent to the cascade. We observe that this type of sequence constitutes a route to chaos. The structures of periods in the hundreds are notable,

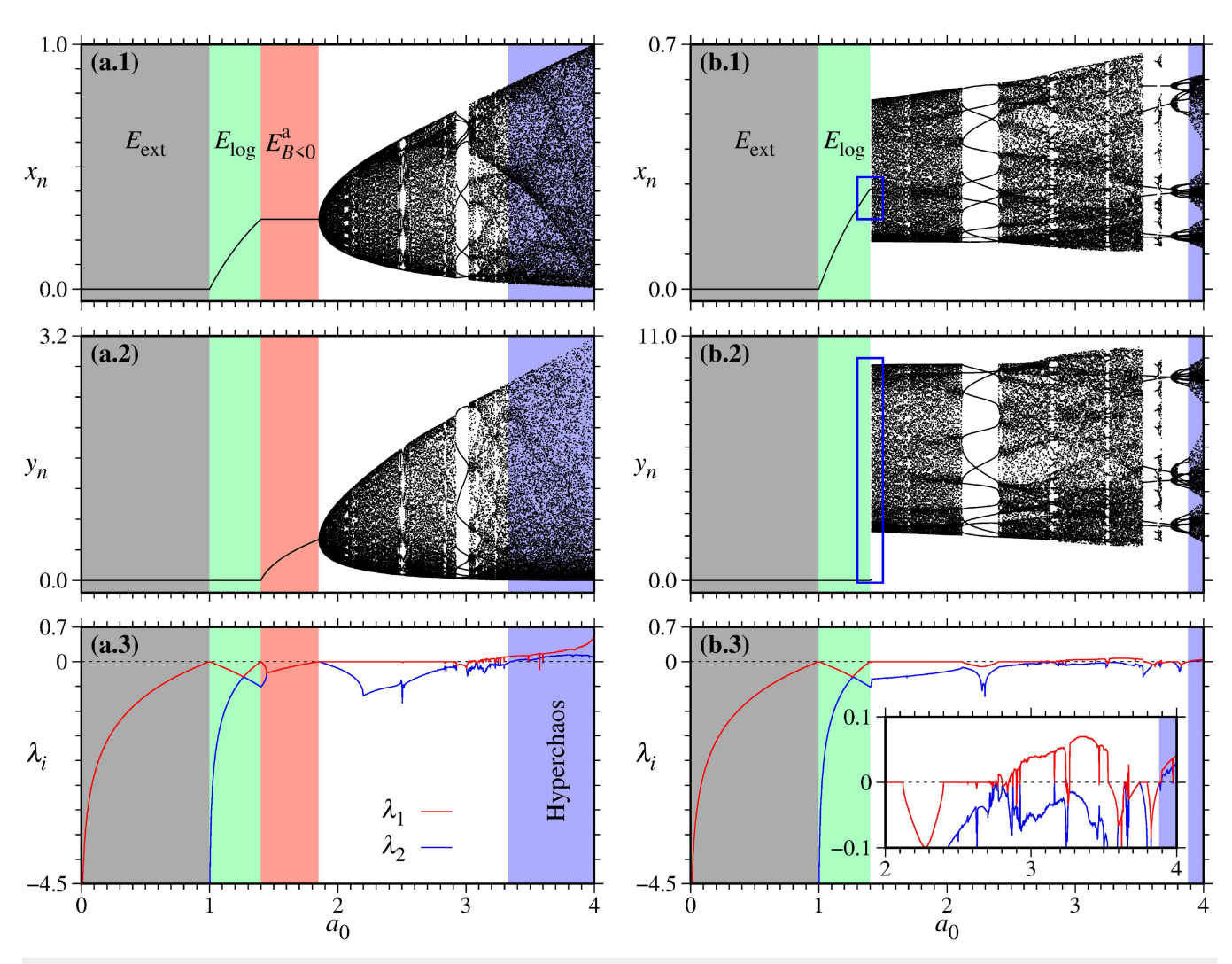


FIG. 8. Bifurcation diagrams along the dashed lines in Fig. 3, accompanied by the respective Lyapunov spectra (on bottom panels). Left panels correspond to $s_1: a_r = 0.5$ and right ones to $s_2: a_r = 3.3$. The interval $0 < a_0 \le 4$ is uniformly discretized by 2000 points. Plotted up to 50 orbit points, after the transient, for each control parameter value. Vertical stripes in the background correspond to the different attractive fixed point intervals: E_{ext} in gray, E_{log} in light green, and $E_{B<0}^a$ in pink. The occurrence of hyperchaos is highlighted by the purple background. (a.1-2) A quasiperiodic orbit emerges, in $a_0 \approx 1.85$, from the point in scenario (iii) via a Neimark–Sacker bifurcation. (a.3) Hyperchaos arises from chaos with the slow growth of the second Lyapunov exponent. (b.1-2) Sudden change from a fixed point to a quasiperiodic orbit. The region highlighted by the blue box is enlarged in Fig. 9, where the existence of a scenario (iii) equilibrium point is verified. (b.3) Hyperchaos emerges abruptly with the rapid growth of both Lyapunov exponents. The range $2 < a_0 \le 4$ is expanded in the inset, allowing a better distinction of the exponent values.

such as p=192 (blue) bifurcating to 384 (light green). Also, p=104 (yellow) bifurcating to 208 (light blue), and others, such as p=224 (brown) in the doubling cascade from p=56 (green). As in Fig. 5, there are tongues starting from the quasiperiodic region and advancing toward the chaotic one, continuing the alternation between the periodic and quasiperiodic regimes.

Panel (c) enlarges the highlighted box in the lower right corner of (b). We focus on the structures inserted in the quasiperiodic strip internal to the period-56 region. We observe an area of chaos partially outlined by the quasiperiodic band and below delimited by

the p=56 band. There are pairs of connected Arnold tongues of the same period, whose link crosses the chaotic region, with the structures on the left (around $a_0=3.264$) highly distorted. What can be seen in the cases p=336 (pink) and p=392 (dark blue). The period along these Arnold tongues sequence is incremented with accumulation at p=56. To describe the rule of periods corresponding to this formation, it is necessary to multiply the denominators in the Farey sequence by the accumulation factor 56. We selected a region on the right of Fig. 6(c) to investigate the presence of periodic structures immersed in small chaotic domains, which are delimited by

the narrow periodic stripes from the Arnold tongues. This region is studied in Fig. 7(a).

Unlike the similar structures shown in Fig. 5, in the panel of Fig. 7, it can be seen that all tongues, from the quasiperiodic region, advance to the chaotic one where a period-doubling bifurcation occurs. There are no bifurcations of these periodic structures for quasiperiodic behavior in the direction to chaos. As examples, the doubling from p=448 (violet color) to 896 (light brown) in the upper left corner and from p=504 (magenta) to 1008 (light blue) in the central region of the picture. Note that unlisted periods multiple of 56 are represented in cyan (P56). In this enlargement, it is clear that the periods of the main part of primary structures add 56 units following the direction of decreasing a_r and increasing a_0 . As well, a general rule for period formation is obtained from the denominators in the Farey sequence multiplied by 56. We leave the example of the period 952 tongue (petrol blue), intermediate between p=448 and p=504.

All periodic stripes prolonging from the tongues to the chaotic regions intersect forming a net, which subdivides the plane into small chaotic domains. 60,62 Each part of this megastructure resembles a quadrilateral, whose vertices are located at the intersections of the periodic stripes. In the grid formed, multistability occurs, with different pairs of attractive orbits coexisting at each intersection. Immersed in every chaotic subdomain, there is a main shrimp accompanied by periodic satellite structures. Given that this megastructure has a net shape and encloses areas with immersed shrimp, we suggestively refer to it by the term "shrimp fisher." The box highlighted in panel (a) is enlarged in (b), where the "fished" shrimps can be seen more clearly. The rule for increasing the periods of these main shrimps occurs in two directions, 62 as indicated by the arrows in the illustration. Starting from the period-1008 shrimp (blue), located around $a_r = 3.26865$ and $a_r = 1.25092$, and advancing in the direction of both parameters increase, we find the shrimp of p = 1064 (pink). A structure of the same period is found in the direction of a_r decrease. Following this rule, we get the periods of all shrimps in the "shrimp fisher."

Attractive equilibrium points occur in different scenarios within the large period-1 region, subject discussed in Sec. III. The change of a fixed-point type can be seen in Fig. 8, which presents bifurcation diagrams along two parallel to axis a_0 , namely, the lines $s_1: a_r = 0.5$ and $s_2: a_r = 3.3$ (both dashed lines in Fig. 3). We also observe the transition from chaos to hyperchaos, as well as the quasiperiodic behavior emergency via a Neimark-Sacker bifurcation. Figures 8(a.1) and 8(a.2) consist of the bifurcation diagrams along s_1 for the system's variables x and y, respectively. The panel (a.3) displays the corresponding Lyapunov spectrum. By the background colors, we draw attention to the domain of each stable fixed point. Logistic map solutions are verified for the base growth parameter interval $0 < a_0 < d/(d-1) = 1.4$, where predator's population goes to zero. Mutual extinction occurs for $0 < a_0 < 1$ (gray background), and after a transcritical bifurcation at a = 1, a stable prey-only scenario emerges (light-green background). The point E_{log} becomes unstable from $a_0 = 1.4$, arising a constant population balance between prey and predator (pink background). This equilibrium is of the first type (a) for B < 0, i.e., a unique solution with $a_0>1.4$. Finally, $E^a_{B<0}$ is unstable from $a_0\approx 1.85$, where a Neimark-Sacker bifurcation occurs giving rise to the quasiperiodic

region. The largest Lyapunov exponent λ_1 [red curve in Fig. 8(a.3)] corroborates the bifurcation diagram, reaching zero level in the stability changes, and remaining null within the quasiperiodic band. The periodic windows amid the aperiodic behavior correspond to the intersection of the line s_1 with the tongues seen in Fig. 3, such as the wide period-11 interval around $a_0 = 3$. We highlight the hyperchaotic band (purple background), which starts approximately at $a_0 = 3.35$ from chaos and presents high density of points between $y_n = 0$ and $y_n = 0.4$.

The right panels of Figure 8 show the attractive solutions along the line s_2 . For $a_0 < 1.4$, the behavior is indistinct from that seen over s_1 in the left panels. At $a_0 \approx 1.4$, an abrupt transition from a fixed point to a quasiperiodic orbit is observed. This happens because the Neimark-Sacker bifurcation is in another direction, from the point $E_{B<0}^a$. We highlight the intermediate interval (blue border box) between the stable E_{log} and the aperiodic orbit. In this narrow range, there is a stable equilibrium point of species coexistence, best seen in Fig. 9. Notable is the period-13 window around $a_0 \approx 2.25$, corresponding to the intersection of s_2 with the lightgreen area in Fig. 3. The inset on the panel (b.3) shows a chaos region from $a_0 \approx 2.8$ to $a_0 \approx 3.6$ and the hyperchaos band starting at $a_0 \approx 3.9$ (purple background). In this, there are small exponents $\lambda_{1,2} > 0$ occurring after a periodic window subsequent to a little quasiperiodic range. Unlike the gradual emergence of hyperchaos over s_1 , which occurs in the sequence of fixed point \rightarrow quasiperiodicity \rightarrow chaos \rightarrow hyperchaos, in s_2 , such dynamics suddenly arise

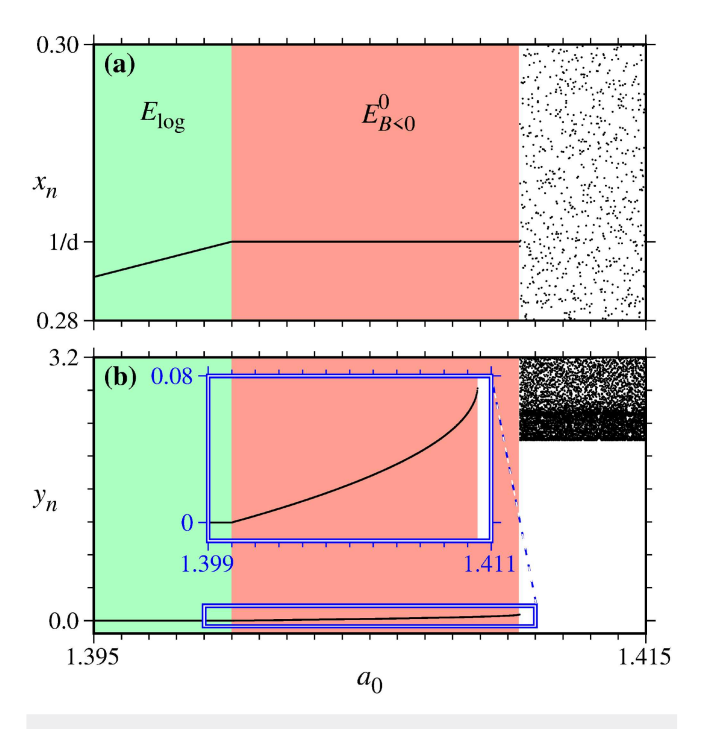


FIG. 9. Magnifications inside the highlighted boxes in Fig. 8(a.1-2), focusing on the narrow range of the stable fixed point $E_{B<0}^0$ (pink background). (a) The change in the fixed point type is observed at $a_0=1.4$. (b) The small predator population values are best seen in the inset.

with the simultaneous growth of both Lyapunov exponents. The line $a_r = 3.3$ intersects the period-6 strip (orange in Fig. 3) from $a_0 \approx 3.4$ to $a_0 \approx 3.75$, where the periodic orbit becomes unstable via a Neimark-Sacker bifurcation. After the quasiperiodic region, there is a high-period window and the subsequent sudden growth of both $\lambda_{1,2}$.

An intermediate band between the logistic equilibrium and the quasiperiodic region is identified along the line s_2 by means of the magnifications shown in Fig. 9. This enlargement considers an internal segment to the highlighted box in Fig. 8(b.1-2). The stable fixed point $E_{R<0}^0$ (pink background) arises from $a_0 = 1.4$, when the logistic solution becomes unstable, remaining until $a_0 \approx 1.4104$, where a region of attractive quasiperiodic orbits abruptly occurs. In panel (a), we draw attention to the fact that $x_* = 1/d$ in the domain of $E_{B<0}^0$, corroborating that it is a fixed point in scenario (iii). The inset in panel (b) confirms $y_* \neq 0$ on an upward-sloping curve in the same interval.

V. CONCLUSIONS

By analytical and numerical investigations, we show that the prey-predator model with reproductive responsiveness of prey can evolve into three different scenarios: mutual extinction, extinction of predators only, and coexistence of species. The stability of equilibrium points for which the predator population vanishes does not depend on the responsive growth parameter, as well as the mutual extinction is determined solely by the base growth parameter. The dynamics in the coexistence scenario are strongly dependent on the responsive parameter.

Quasiperiodic, chaotic, and hyperchaotic behaviors were found as a function of both prey population growth parameters. We identified Arnold tongue-like periodic structures inserted in stripes of quasiperiodicity and organized in the well-known period formation rule according to the denominators of the Farey sequence. Periodic connected structures have also been studied, such as pairs of twin shrimps and linked Arnold tongues. We highlight the net-shaped megastructure formed by the successive crossings of periodic bands extended from the Arnold tongues, which is associated with the occurrence of shrimps in a period formation rule in two directions in the parameter plane. Thus, we found that the prey-predator model with a responsive prey reproduction factor presents rich dynamics in both prey reproductive strategies, either increasing or decreasing the population growth rate in response to predation risk.

ACKNOWLEDGMENTS

The authors acknowledge the financial support from the Coordination for the Improvement of Higher Education Personnel (CAPES) under Grant No. 88887.951599/2024-00, the São Paulo Research Foundation (FAPESP, Brazil) under Grant Nos. 2021/12232-0 and #2018/03211-6, and the Brazilian National Council for Scientific and Technological Development (CNPq) (No. 304616/2021-4).

AUTHOR DECLARATIONS

Conflict of Interest

The authors have no conflicts to disclose.

Author Contributions

M. S. Bittencourt: Formal analysis (equal); Investigation (equal); Software (equal); Validation (equal); Writing - original draft (equal); Writing - review & editing (equal). E. L. Brugnago: Conceptualization (equal); Data curation (equal); Formal analysis (equal); Investigation (equal); Methodology (equal); Software (equal); Validation (equal); Writing - original draft (equal); Writing - review & editing (equal). Z. O. Guimarães-Filho: Supervision (equal); Writing SSİ review & editing (equal). I. L. Caldas: Project administration (equal); Resources (equal); Writing - review & editing (equal). A. S. Reis: Conceptualization (equal); Formal analysis (equal); Investigation (equal); Methodology (equal); Project administration (equal); Supervision (equal); Writing – original draft (equal); Writing – review & editing (equal).

DATA AVAILABILITY

The data that support the findings of this study are available from the corresponding author upon reasonable request.

REFERENCES

- ¹T. R. Malthus, An Essay on the Principle of Population (Reeves and Turner, London, 1878).
- ²A. J. Lotka, Analytical Theory of Biological Populations (Springer Science & Business Media, 1998).
- ³N. Bacaër, A Short History of Mathematical Population Dynamics (Springer, 2011), Vol. 618.
- ⁴L. Euler, *Introductio in Analysin Infinitorum* (MM Bousquet, 1748), Vol. 2.
- ⁵P.-F. Verhulst, "Recherches mathématiques sur la loi d'accroissement de la population," Mém. l'Acad. r. Belg. 18, 1–40 (1845).

 ⁶P.-F. Verhulst, Deuxième Mémoire sur la Loi d'accroissement de la Population
- (Hayez, 1847), Vol. 269.
- ⁷D. Tilman, "The importance of the mechanisms of interspecific competition," Am. Nat. 129, 769-774 (1987).
- ⁸P. Chesson and J. J. Kuang, "The interaction between predation and competition," Nature 456, 235-238 (2008).
- ⁹K. Burns and P. Lester, "Competition and coexistence in model populations," in Encyclopedia of Ecology (Academic Press, Oxford, 2008), pp. 701–707.
- ¹⁰W. J. Ripple and R. L. Beschta, "Trophic cascades in Yellowstone: The first 15 years after wolf reintroduction," Biol. Conserv. 145, 205–213 (2012).

 11 A. J. Lotka, "Analytical note on certain rhythmic relations in organic systems,"
- Proc. Natl. Acad. Sci. U.S.A. 6, 410-415 (1920).
- ¹²A. J. Lotka, Elements of Physical Biology (Williams & Wilkins, 1925).
- ¹³V. Volterra, "Variazioni e fluttuazioni del numero d'individui in specie animali conviventi," Memor. Accad. Lincei, Ser. 6, 31-113 (1926).
- ¹⁴V. Volterra, "Fluctuations in the abundance of a species considered mathematically," Nature 118, 558-560 (1926).
- 15 J. Hofbauer and K. Sigmund, "Lotka-Volterra equations for predator-prey systems," in Evolutionary Games and Population Dynamics (Cambridge University Press, 1998), pp. 11-21.
- ¹⁶Y. Takeuchi, Global Dynamical Properties of Lotka-Volterra Systems (World Scientific, 1996).
- ¹⁷J. G. Freire, M. R. Gallas, and J. A. C. Gallas, "Impact of predator dormancy on
- prey-predator dynamics," Chaos **28**, 053118 (2018).

 ¹⁸V. A. Kuznetsov, I. A. Makalkin, M. A. Taylor, and A. S. Perelson, "Nonlinear dynamics of immunogenic tumors: Parameter estimation and global bifurcation analysis," Bull. Math. Biol. 56, 295-321 (1994).
- ¹⁹L. G. De Pillis and A. Radunskaya, "The dynamics of an optimally controlled tumor model: A case study," Math. Comput. Model. 37, 1221-1244 (2003).
- ²⁰M. R. Gallas, M. R. Gallas, and J. A. C. Gallas, "Distribution of chaos and periodic spikes in a three-cell population model of cancer," Eur. Phys. J. Spec. Top. 223, 2131-2144 (2014).

- ²¹R. M. May, "Simple mathematical models with very complicated dynamics," Nature **261**, 459–467 (1976).
- $^{22}\mathrm{M}.$ J. Feigenbaum, "Universal behavior in nonlinear systems," Physica D 7, 16-39 (1983).
- ²³J. A. C. Gallas, "Nonlinear dependencies between sets of periodic orbits," Europhys. Lett. 47, 649 (1999).
- ²⁴J. E. S. Socolar, "Chaos," in Encyclopedia of Physical Science and Technology, 3rd ed., edited by R. A. Meyers (Academic Press, New York, 2003), pp. 637-665.
- ²⁵J. A. C. Gallas, "Preperiodicity and systematic extraction of periodic orbits of the quadratic map," Int. J. Mod. Phys. C 31, 2050174 (2020).
- ²⁶E. N. Lorenz, "The problem of deducing the climate from the governing
- equations," Tellus 16, 1–11 (1964). ²⁷S. M. Ulam and J. Von Neumann, "On combination of stocastic deterministic
- processes," Bull. AMS 53, 1120 (1947). ²⁸ M. Gyllenberg, G. Söderbacka, and S. Ericsson, "Does migration stabilize local population dynamics? Analysis of a discrete metapopulation model," Math. Biosci. 118, 25-49 (1993).
- ²⁹A. Hastings, "Complex interactions between dispersal and dynamics: Lessons from coupled logistic equations," Ecology 74, 1362-1372 (1993).
- ³⁰ A. L. Lloyd, "The coupled logistic map: A simple model for the effects of spatial heterogeneity on population dynamics," J. Theor. Biol. 173, 217-230 (1995).
- ³¹Y. A. Kuznetsov, Elements of Applied Bifurcation Theory, 4th ed. (Springer,
- 32 P. C. Rech, M. W. Beims, and J. A. C. Gallas, "Generation of quasiperiodic oscillations in pairs of coupled maps," Chaos, Solitons Fractals 33, 1394-1410
- ${\bf ^{33}}$ G. C. Layek and N. C. Pati, "Organized structures of two bidirectionally coupled logistic maps," Chaos 29, 093104 (2019).
- ³⁴J. M. Smith, Mathematical Ideas in Biology (CUP Archive, 1968).
- 35 G. I. Bischi and F. Tramontana, "Three-dimensional discrete-time Lotka-Volterra models with an application to industrial clusters," Commun. Nonlinear ci. Numer. Simul. 15, 3000-3014 (2010).
- ³⁶Q. Din, "Dynamics of a discrete Lotka-Volterra model," Adv. Differ. Equ. 2013,
- 1–13. $^{\bf 37}$ A. Q. Khan and M. N. Qureshi, "Global dynamics and bifurcations analysis of a two-dimensional discrete-time Lotka-Volterra model," Complexity 2018, 7101505.
- 38 R. Shine and T. Madsen, "Prey abundance and predator reproduction: Rats and pythons on a tropical Australian floodplain," Ecology 78, 1078–1086 (1997).

 39 N. P. Anders, "Predator behaviour and prey density: Evaluating density-
- dependent intraspecific interactions on predator functional responses," J. Anim. Ecol. 70, 14-19 (2001).
- $^{\bf 40}{\rm M.~E.~Solomon,}$ "The natural control of animal populations," J. Anim. Ecol. 18, 1-35 (1949).
- ⁴¹V. Křivan, "Prey-predator models," in *Encyclopedia of Ecology*, edited by S. E. Jørgensen and B. D. Fath (Academic Press, Oxford, 2008), pp. 2929-2940.
- ⁴²M. J. Cherry, K. E. Morgan, B. T. Rutledge, L. M. Conner, and R. J. Warren, "Can coyote predation risk induce reproduction suppression in white-tailed deer?" Ecosphere 7, e01481 (2016).
- 43 S. Creel and D. Christianson, "Relationships between direct predation and risk effects," Trends Ecol. Evol. 23, 194-201 (2008).

- 44K. Norrdahl and E. KorpimÄki, "The impact of predation risk from small mustelids on prey populations," Mammal Rev. 30, 147–156 (2000).

 45 G. D. Ruxton and S. L. Lima, "Predator-induced breeding suppression and its
- consequences for predator-prey population dynamics," Proc. R. Soc. Lond., Ser. B **264**, 409–415 (1997).
- ⁴⁶M. Danca, S. Codreanu, and B. Bako, "Detailed analysis of a nonlinear prey-
- predator model," J. Biol. Phys. **23**, 11 (1997).

 ⁴⁷C. S. Holling, "The components of predation as revealed by a study of smallmammal predation of the European pine sawfly," Can. Entomol. 91, 293-320
- ⁴⁸J. Dawes and M. Souza, "A derivation of Holling's type I, II and III functional responses in predator–prey systems," J. Theor. Biol. 327, 11–22 (2013). 49 E. L. Lima, "A equação do terceiro grau," Mat. Univ. 5, 10–23 (1987).
- ⁵⁰K. Alligood, T. Sauer, and J. Yorke, Chaos: An Introduction to Dynamical
- Systems, Textbooks in Mathematical Sciences (Springer, New York, 1996).
 51 J.-P. Eckmann and D. Ruelle, "Ergodic theory of chaos and strange attractors," Rev. Mod. Phys. 57, 617 (1985).
- 52G. Benettin, L. Galgani, A. Giorgilli, and J.-M. Strelcyn, "Lyapunov characteristic exponents for smooth dynamical systems and for Hamiltonian systems; a method for computing all of them. Part 1: Theory," Meccanica 15, 9-20 (1980).
- 53 G. Benettin, L. Galgani, A. Giorgilli, and J.-M. Strelcyn, "Lyapunov characteristic exponents for smooth dynamical systems and for Hamiltonian systems; a method for computing all of them. Part 2: Numerical application," Meccanica 15, 21-30 (1980).
- 54T. Kapitaniak, Y. Maistrenko, and S. Popovych, "Chaos-hyperchaos transition," Phys. Rev. E 62, 1972 (2000).
- 55 G. H. Hardy and E. M. Wright, An Introduction to the Theory of Numbers (Oxford University Press, 1979).
- ⁵⁶ "Small denominators. I. Mapping of the circumference onto itself," in Collected Works: Representations of Functions, Celestial Mechanics and KAM Theory, 1957-1965, edited by A. B. Givental, B. A. Khesin, J. E. Marsden, A. N. Varchenko, V. A. Vassiliev, O. Y. Viro, and V. M. Zakalyukin (Springer, Berlin, 2009),
- pp. 152–223.

 ⁵⁷P. C. Rech, "Organization of the periodicity in the parameter-space of a glycol-
- ysis discrete-time mathematical model," J. Math. Chem. 57, 632–637 (2019). ⁵⁸J. A. Gallas, "Structure of the parameter space of the Hénon map," Phys. Rev. Lett. 70, 2714 (1993).
- 59 R. Vitolo, P. Glendinning, and J. A. Gallas, "Global structure of periodicity hubs in Lyapunov phase diagrams of dissipative flows," Phys. Rev. E 84, 016216 (2011). 60 G. M. Ramírez-Ávila and J. A. C. Gallas, "How similar is the performance of the cubic and the piecewise-linear circuits of Chua?" Phys. Lett. A 375, 143-148
- ⁶¹S. L. de Souza, I. L. Caldas, R. L. Viana et al., "Multistability and self-similarity in the parameter-space of a vibro-impact system," Math. Probl. Eng. 2009, 290356 (2009).
- 62 S. L. de Souza, A. A. Lima, I. L. Caldas, R. O. Medrano-T, and Z. D. O. Guimarães-Filho, "Self-similarities of periodic structures for a discrete model of a two-gene system," Phys. Lett. A 376, 1290-1294 (2012).
- 63 C. Bonatto, J. C. Garreau, and J. A. Gallas, "Self-similarities in the frequencyamplitude space of a loss-modulated CO2 laser," Phys. Rev. Lett. 95, 143905